

## Supplementary data

### Versatility of pyridoxal phosphate as a coating of iron oxide nanoparticles

Debora Bonvin,<sup>1</sup> Ulrich Aschauer,<sup>2</sup> Jessica A.M. Bastiaansen,<sup>3,4</sup> Matthias Stuber,<sup>3,4</sup> Heinrich Hofmann,<sup>1</sup> and Marijana Mionić Ebersold<sup>1,3,4\*</sup>

<sup>1</sup>Powder Technology Laboratory, Insitute of Materials, Ecole polytechnique fédérale de Lausanne, Switzerland.

<sup>2</sup>Department of Chemistry and Biochemistry, University of Bern, Bern, Switzerland.

<sup>3</sup>Department of Radiology, University Hospital (CHUV) and University of Lausanne (UNIL), Switzerland.

<sup>4</sup>Center of Biomedical Imaging (CIBM), Lausanne, Switzerland.

\*Corresponding author E-mail addresses: marijanamionic@gmail.com; Marijana.Mionic-Ebersold@chuv.ch.

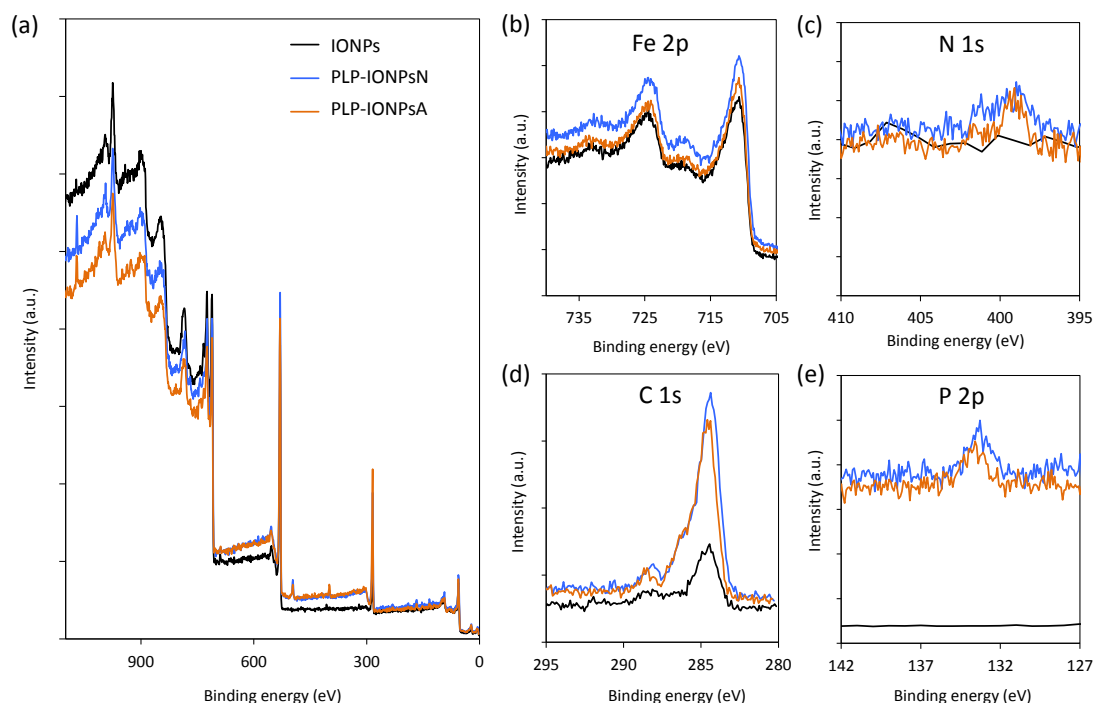


**Fig. S1:** Overall XPS spectra of uncoated IONPs, PLP-IONPsN and PLP-IONPsA (a), as well as their Fe 2p (b), N 1s (c), C 1s (d) and P 2p (e) peaks.

**Table S1:** Atomic percentages of Fe, O, C and N obtained by XPS in uncoated IONPs, PLP-IONPsN and PLP-IONPsA.

Atomic %	Fe 2p	O 1s	C 1s	N 1s	P 2p
IONPs	32.0	50.6	17.3	-	-
PLP-IONPsN	21.9	43.0	32.0	2.1	1.1
PLP-IONPsA	18.6	44.3	33.6	2.2	1.3

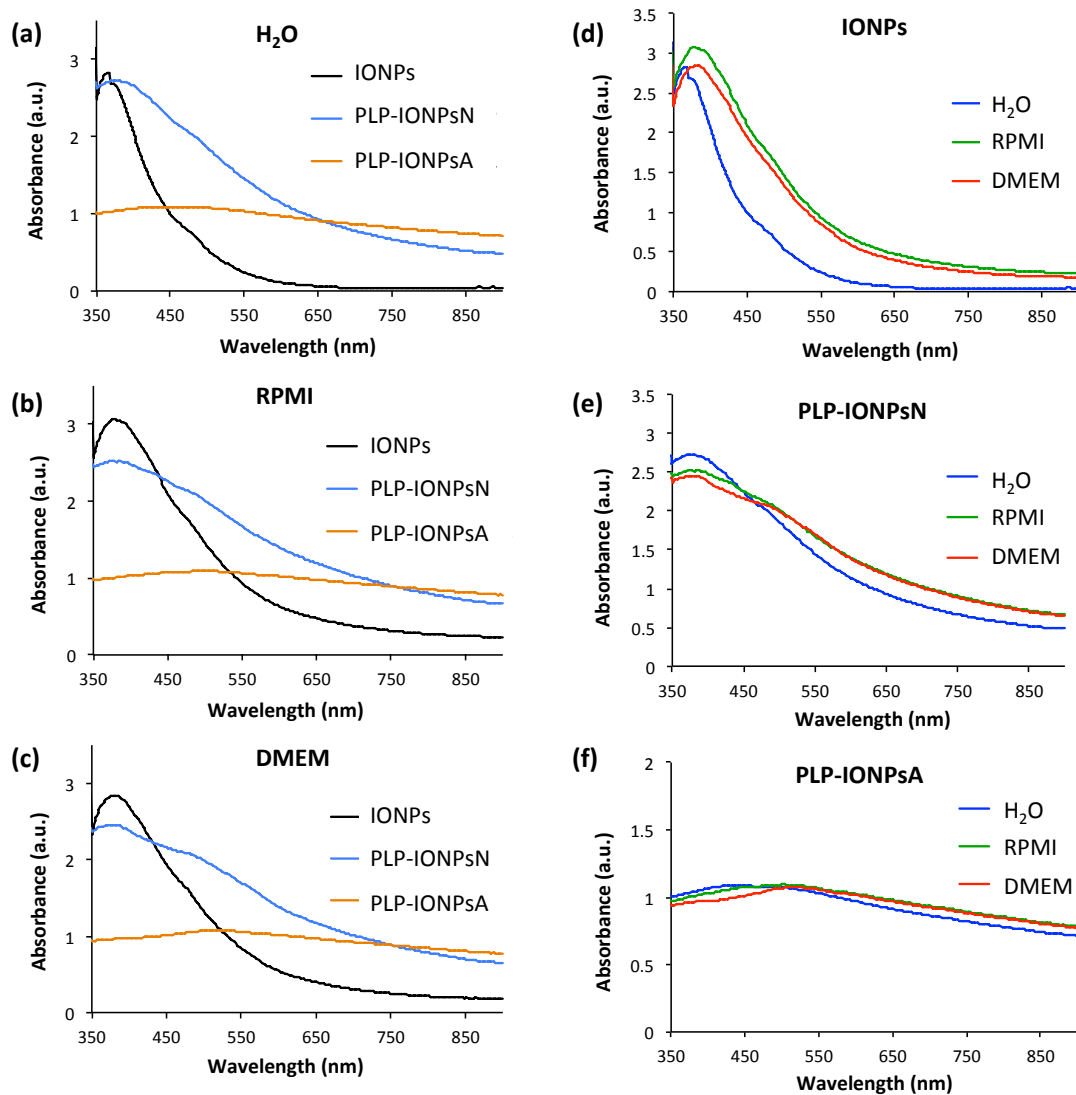


**Fig. S2:** Absorbance measured by UV-visible spectroscopy in H<sub>2</sub>O (a), in RPMI medium (b) and in DMEM (c) of uncoated IONPs (d), PLP-IONPsN (e) and PLP-IONPsA (f).

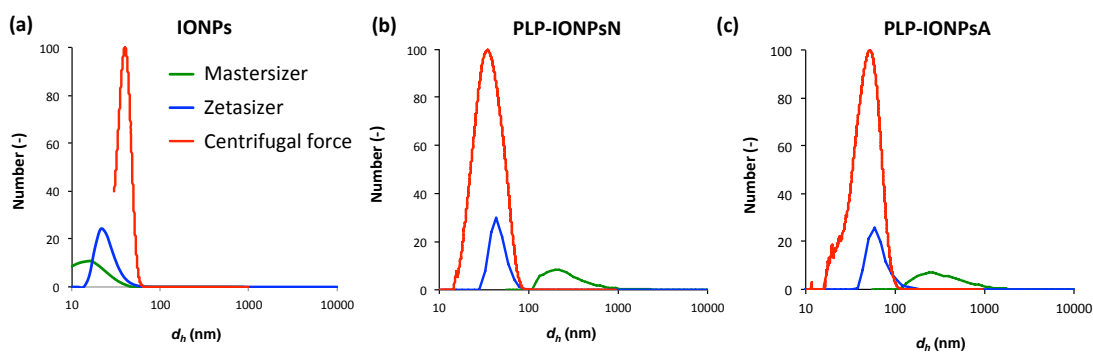


**Fig. S3:** Number weighted distribution of the hydrodynamic diameter,  $d_h$ , of uncoated IONPs (a), PLP-IONPsN (b), and PLP-IONPsA (c) measured by dynamic light scattering with the two instruments (Mastersizer or Zetasizer), or by centrifugal force.

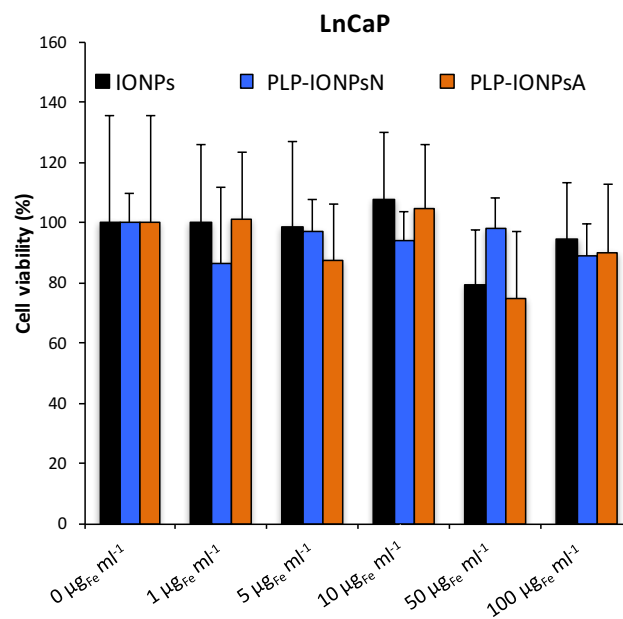


**Fig. S4:** Viability of LnCaP cells incubated for 24 h with different concentrations (0, 5, 10, 50 and 100  $\mu\text{g}_{\text{Fe}} \text{ml}^{-1}$ ) of uncoated IONPs, PLP-IONPsN and PLP-IONPsA measured with the MTS assay. The cell viabilities are percentages of viable cells treated with IONPs normalized with the number of viable cells without IONPs (0  $\mu\text{g}_{\text{Fe}} \text{ml}^{-1}$ ).

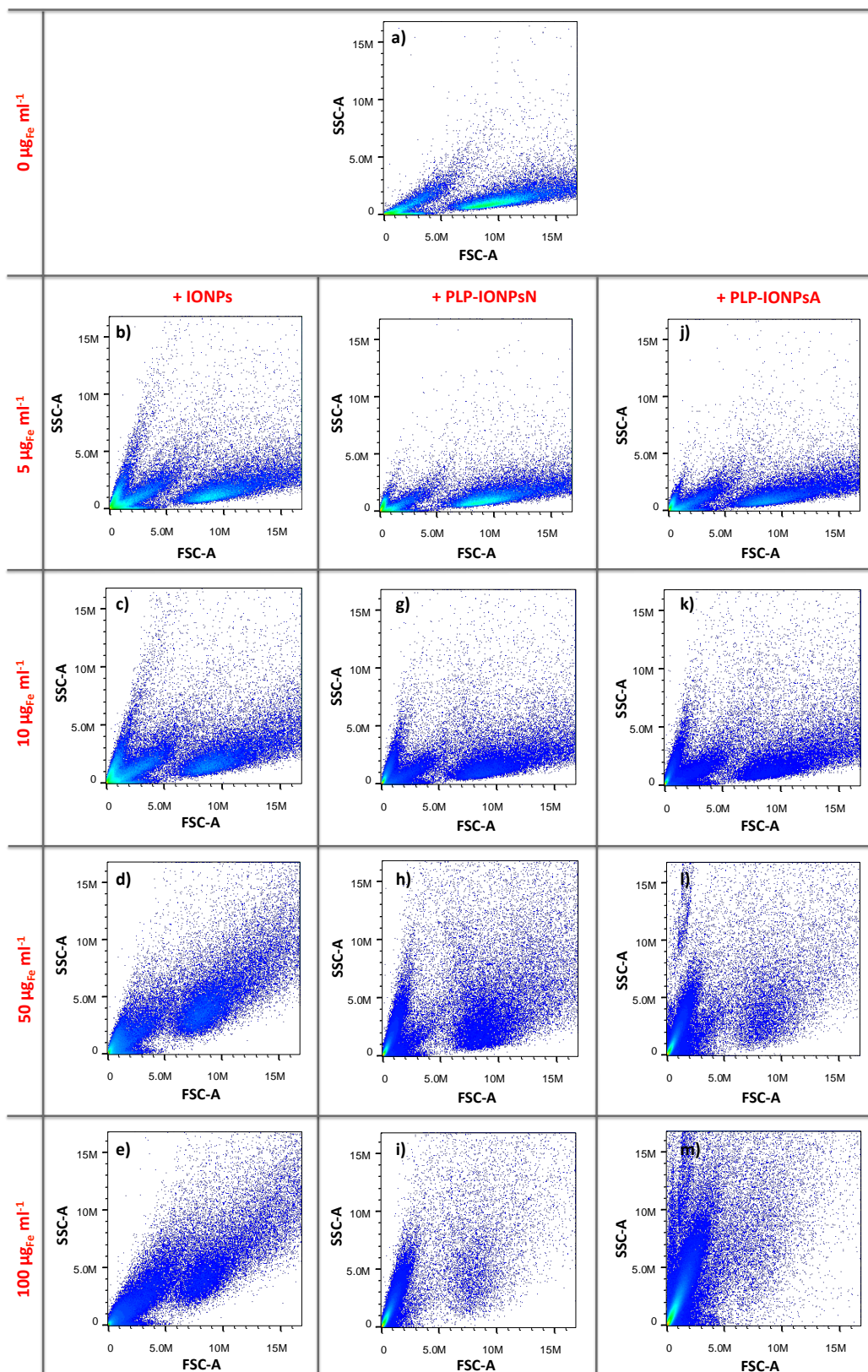


**Fig. S5:** Forward scatter (FSC) vs side scatter (SSC) plot of LnCaP cells without IONPs ( $0 \mu\text{g}_{\text{Fe}} \text{ml}^{-1}$ ; a) or treated for 24 h with different concentrations (5, 10, 50 and  $100 \mu\text{g}_{\text{Fe}} \text{ml}^{-1}$ ) of uncoated IONPs (b, c, d, e), PLP-IONPsN (f, g, h, i) or PLP-IONPsA (j, k, l, m). SSC-A and FSC-A = area of the side and forward light scatter pulse. Data from a selected experiment.

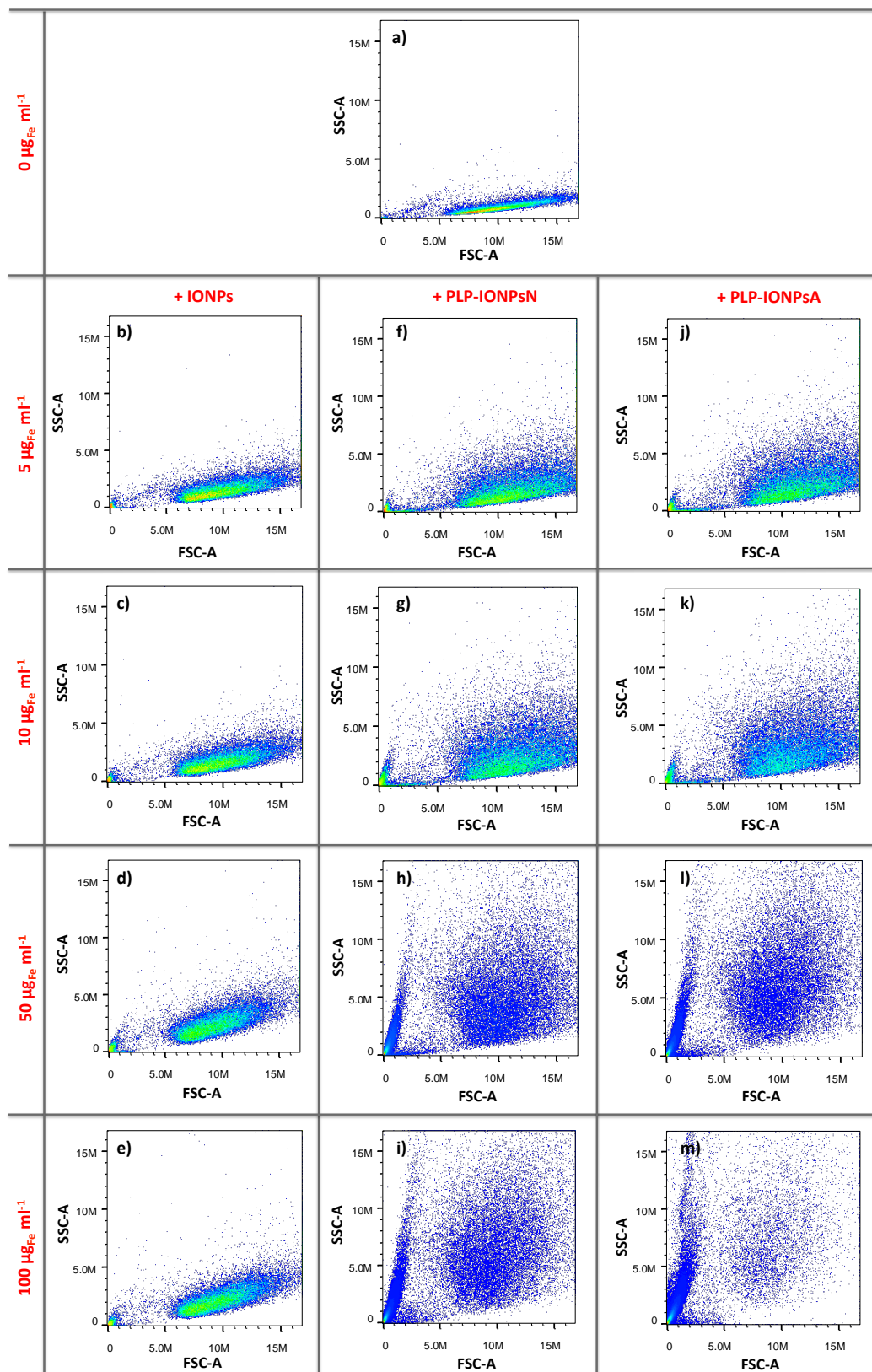


**Fig. S6:** Forward scatter (FSC) vs side scatter (SSC) plot of PC3 cells without IONPs ( $0 \mu\text{g}_{\text{Fe}} \text{ ml}^{-1}$ ; a) or treated for 24 h with different concentrations (5, 10, 50 and  $100 \mu\text{g}_{\text{Fe}} \text{ ml}^{-1}$ ) of uncoated IONPs (b, c, d, e), PLP-IONPsN (f, g, h, i) or PLP-IONPsA (j, k, l, m). SSC-A and FSC-A = area of the side and forward light scatter pulse. Data from a selected experiment.

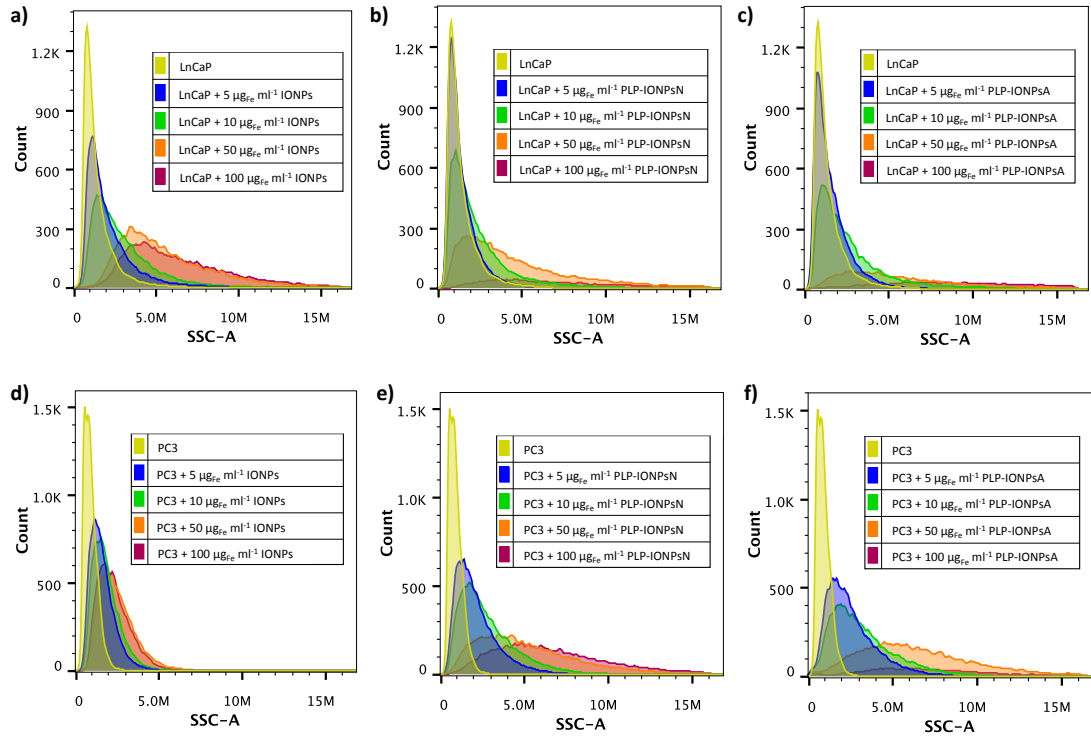


**Fig. S7:** Counts vs area of the side scatter (SSC-A) plot of LnCaP (a, b, c) and PC3 (d, e, f) cells treated for 24 h with different concentrations (5, 10, 50 and 100  $\mu\text{g}_{\text{Fe}} \text{ml}^{-1}$ ) of uncoated IONPs (a, d), PLP-IONPsN (b, e) and PLP-IONPsA (c, f). Data from experiments selected in Fig. S4 and S5.

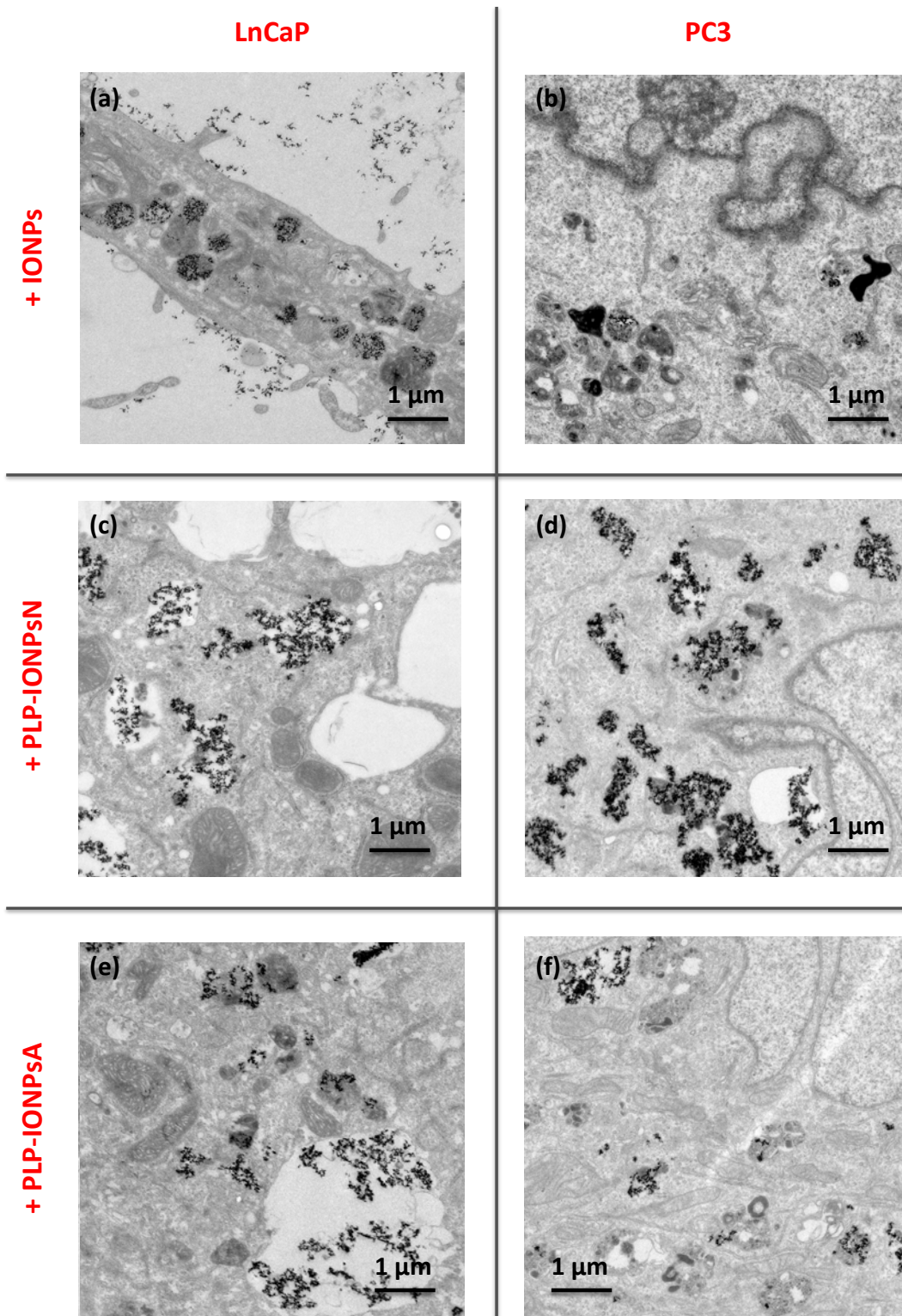


**Fig. S8:** Representative TEM micrographs of 50 nm-thick cross-sections of LnCaP cells (a, c, e) and PC3 cells (b, d, f) incubated with uncoated IONPs (a, b), PLP-IONPsN (c, d) and PLP-IONPsA (e, f) and embedded in resin.